Crack path prediction in layered ceramics designed with residual stresses

O. Ševeček[1], R. Bermejo[2] and M. Kotoul[3]

[1] Materials Center Leoben Forschung GmbH, Roseggerstraße 12, 8700 Leoben, Austria, Email: sevecek@seznam.cz

[2] Montanuniversität Leoben , Institut für Struktur- und Funtionskeramik, Peter-Tunner Straße 5, 8700 Leoben, Austria. Email: raul.bermejo@unileoben.ac.at

[3] Brno University of Technology, Institute of Solid Mechanics, Mechatronics and Biomechanics, Faculty of Mechanical Engineering, Technická 2, 616 69 Brno, Czech Republic, Email: kotoul@fme.vutbr.cz

ABSTRACT. *In this work a computational tool, aiming to predict the crack propagation (i.e. straight propagation, single deflection or bifurcation) in layered ceramics designed with internal residual stresses, is developed. They consist of two material layers with different properties, alternated in a multilayer structure. The internal stresses developed during sintering are associated with the thermal expansion mismatch between adjacent layers and volume ratio between both materials. The computational model is based on Finite Fracture Mechanics theory, especially focused on cracks terminating at the interface between two different material layers. The method utilizes a matched asymptotic procedure to derive the change of potential energy associated with the fracture process. The crack follows the path which maximizes the energy released in the fracture process. A combined loading (thermal and mechanical) is taken into consideration to clarify the influence of the residual stresses on the crack path during fracture. The results predicted by the proposed fracture criterion are in good agreement with the experimental observations on the real laminate.*

INTRODUCTION

Layered ceramics have become an alternative choice for the design of structural ceramics with improved fracture toughness and mechanical reliability. The brittle fracture of monolithic ceramics has been overcome by introducing layered architectures of different kind, *i.e.* geometry, composition of layers, residual stresses, weak interfaces, etc. The main goal of such layered ceramics has been to enhance the fracture energy of the system. Among the various laminate designs reported in literature, two main approaches regarding the fracture energy of the interfaces must be highlighted. On the one hand, laminates designed with weak interfaces have been reported to yield significant enhanced failure resistance through interface delamination [1-8]. The fracture of the first layer is followed by crack propagation along the interface, the so-

called "*graceful failure*", preventing the material from catastrophic failure. On the other hand, laminates designed with strong interfaces have shown significant crack growth resistance (R-curve) behaviour through microstructural design (*e.g.* grain size, layer composition) [9-12] and/or due to the presence of compressive residual stresses, acting as a barrier ("*flaw tolerant*") to crack propagation [3,13-20].

The increase in fracture energy in these laminates is associated with energy dissipating mechanisms such as crack deflection/bifurcation phenomena, which act during crack propagation. The optimisation of the layered design is based on the capability of the layers to deviate the crack from straight propagation. Experimental observations have shown the tendency of a crack to propagate with an angle through the compressive layer and even cause delamination of the interface [21] (see Fig. 1). The magnitude of compressive stresses can influence the angle of propagation and subsequent delamination of the interface.
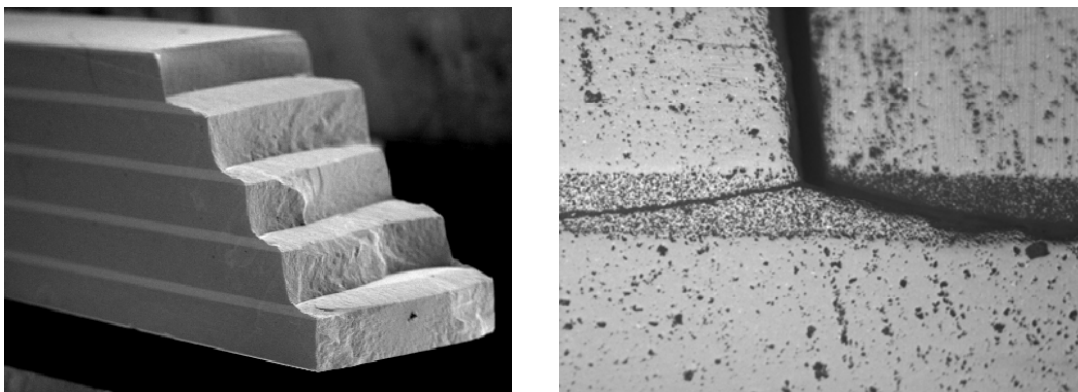

Figure 1. (left) Fracture of a layered ceramic system under flexural bending; bright layers have compressive residual stresses. (right) Bifurcation of a crack entering the first compressive layer of the laminate.

The prediction of the crack path upon loading in such layered systems may help in tailoring the design with maximal fracture energy. Methods based on energetic considerations are available which attempt to predict the behaviour of a crack approaching the interface of dissimilar materials (see for instance [22]). However, the modelling of the propagation of an interface crack through the layered architecture with residual stresses is still missing. A method which can be used to predict the conditions under which the crack will deflect or bifurcate within the compressive layer is sought. In this work, a model based on the finite fracture mechanics approach is developed to interpret and predict the direction of propagation of a crack impinging an interface of a multilayered ceramic designed with internal residual stresses. The thermal strains in the layers occurring during sintering, which are responsible for the mechanical behaviour of the laminate, are taken into account in the model.

MECHANICAL BEHAVIOUR OF A CERAMIC LAMINATE DESIGNED WITH RESIDUAL STRESSES

The mechanical behaviour of a layered ceramic composed of thin layers of Al_2O_3 with 30% monoclinic ZrO_2 (referred to as AMZ layers), sandwiched between thicker layers of Al_2O_3 with 5% tetragonal ZrO_2 (ATZ layers) was tested under the four–point bending. The volume ratio between the AMZ and ATZ material, i.e. V_{AMZ}/V_{ATZ}, was ca. 1/6. The properties of both materials were determined in monolithic samples [19] and are listed in Table 1.

Table 1. Material properties of the laminate components

Material	E [GPa]	ν [-]	$\alpha \times 10^6$ [K^{-1}]	σ_f [MPa]	K_{Ic} [MPa.m$^{1/2}$]	G_c [J/m^2]
ATZ	390±10	0.22	9.8±0.2	422±30	3.2±0.1	25±2
AMZ	280±10	0.22	8±0.2	90±20	2.6±0.1	23±2

In order to investigate the crack propagation in the laminate, a sharp notch of depth 300μm and tip radius of ca. 25 μm, was introduced in the first ATZ layer following the standard SEVNB procedure according to ISO 23146. Due to the tensile residual stresses in the first layer a local stress intensity factor at the crack tip overcomed the fracture toughness K_{Ic} of the ATZ layer during the notching process. Thus, a crack between the notch and the first ATZ/AMZ interface originated without any additional mechanical load (see close-up in Fig. 2a). This was the initial state of the specimen (i.e. crack terminating at the first interface).
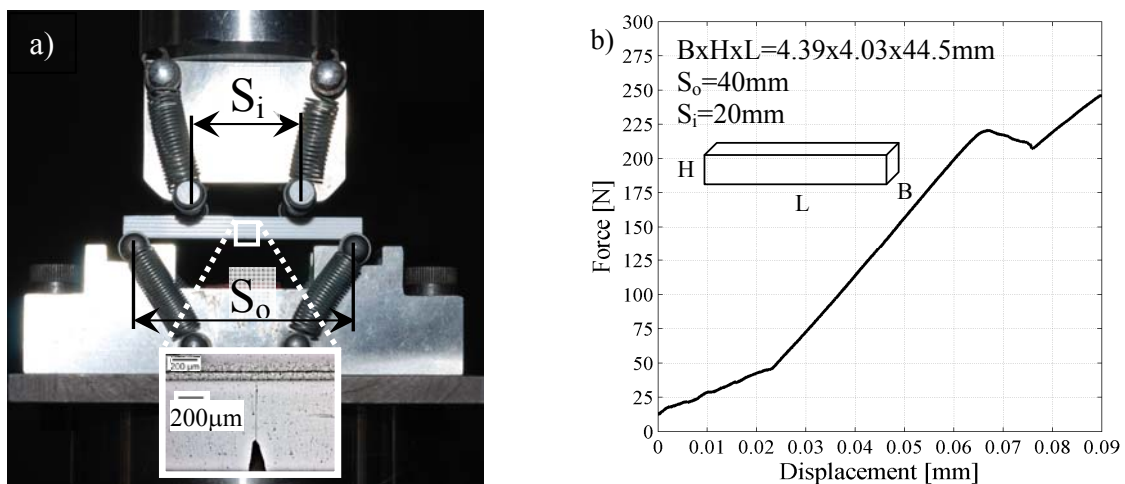

Figure 2. a) Test configuration of the four-point bend experiment on a notched specimen and b) load-displacement curve recorded during testing.

To assess the crack propagation through the laminate, the notched specimen was loaded in four–point bending (inner and outer spans: 20 mm and 40 mm respectively) at a constant displacement rate of 0.5 mm/min using a universal testing machine (Zwick Z010, Switzerland). The testing jig is represented in Fig. 2a. The corresponding load–displacement curve is shown in Fig. 2b.

The first region of the curve (up to 40 N) is associated with the alignment of the rollers during the test. Above 50 N up to 215 N a linear behaviour can be observed: the crack is arrested at the interface until the critical loading force reaches aproximately 220 N. Then a decrease in load can be appreciated, which corresponds to the propagation of the crack through the compressive layer. At this point a sudden crack bifurcation occured and propagation of both cracks branches proceeded towards the next interface. The propagaton angle of the bifurcated crack is shown in Figure 3.
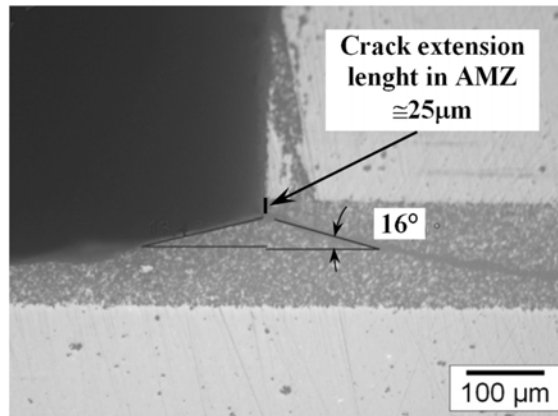

Figure 3. Crack path in the compressive layer of specimen #1.
Picture taken after polishing ca. 250μm from the lateral face of the laminate. Volume ratio of the materials is $V_{AMZ} / V_{ATZ} = 1/6$.

MODEL FOR CRACK PROPAGATION IN CERAMIC LAMINATES BASED ON FINITE FRACTURE MECHANICS

Stress and displacement field description in the vicinity of the crack tip

In order to define a fracture criterion based on the Finite Fracture Mechanics (FFM) approach, an analytical description of the stress field in the vicinity of the crack tip is essential. Especially, crack terminating at the interface of two dissimilar materials is here discussed. Stress field description comprises a calculation of the singularity exponent, determination of the stress and displacement field distribution in the tip vicinity and calculation of the Generalized Stress Intensity Factors (GSIF) as well as the T-stress [23,24]. To calculate singularity exponents and describe the stress field distribution, a Muschelishvili´s solution based on complex potentials has been used. For

the calculations of the Stress Intensity Factors an advantage of the two state integral method (Ψ-integral), based on Betti´s reciprocal theorem, has been utilized [23].

In the following, a symmetric laminate (to avoid bending moments after the cooling process) consisting of 9 alternating ATZ and AMZ layers (the layer from each material has always the same thickness) as used for the experiments is considered for this study.

The singular stress field and displacement field for general stress concentrator are given by the first two terms of the asymptotic expansion:

$$\sigma_{ij} = H_1 \cdot r^{\delta_1-1} \cdot f_{ij1}(\theta) + H_2 \cdot r^{\delta_2-1} \cdot f_{ij2}(\theta),$$
$$\mathbf{U}^0 = H_1 \cdot r^{\delta_1} \cdot \mathbf{u}_1(\theta) + H_2 \cdot r^{\delta_2} \cdot \mathbf{u}_2(\theta)$$

(1)

where H_1 and H_2 are generalized stress intensity factors (GSIF) and δ_1, δ_2 are the corresponding singularity exponents ($\delta_1 < \delta_2$) – see [23, 25]. Functions f_{ij} and $\mathbf{u}_i$, together with the mentioned singularity exponents, are calculated using a method based on the complex potentials. In some particular cases, H_1 is negligible and makes no contribution (e.g. case of a crack perpendicular to the interface under pure mode I of loading). GSIF is calculated using Betti's reciprocal theorem expressed in the form of path independent integral (see [23, 26] and the references herein for more details).

Finite fracture mechanics approach

Since the Energy Release Rate (ERR) for the crack terminating at the interface of two different materials is, for infinitesimally small crack increment, zero or infinite (depending on the singularity type), the classical Griffith approach cannot be applied. To bypass this problem, a theory of Finite Fracture Mechanics (FFM) is applied [27].
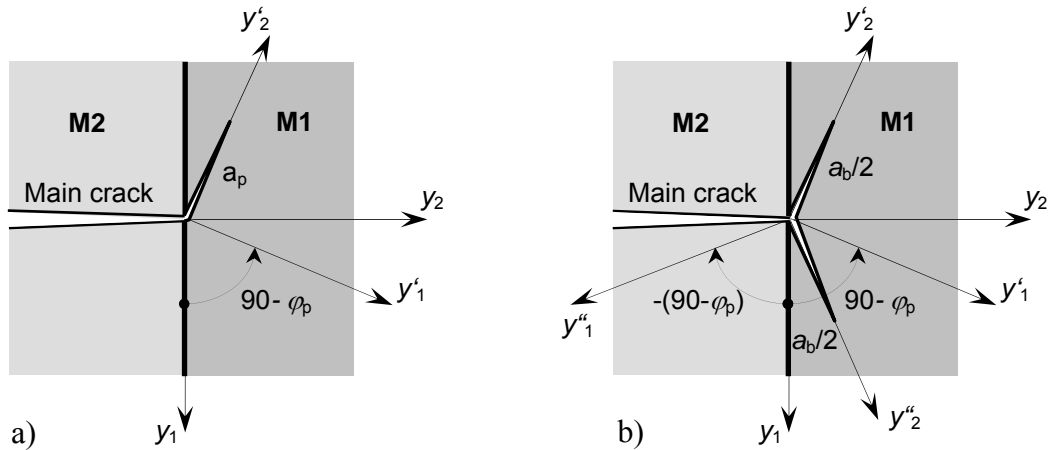

Figure 4. Scheme of a) single crack deflection and b) crack bifurcation (branching) at the interface between materials M2 and M1. A local Coordinate System is defined in the inner domain, where the crack extension length is given as $a_p = a_b/2 + a_b/2$.

Infinitesimal crack increment is substituted by an increment of a finite length and for this increment a change of the potential energy is calculated. The small perturbation parameter ε is defined as $\varepsilon = a_p/W \ll 1$, where W is the characteristic size of the specimen (e.g. specimen height). A second scale to the problem can be introduced, represented by the scaled-up coordinates $(y_1, y_2) = (x_1/\varepsilon, x_2/\varepsilon)$, which provides a zoomed-in view into the region surrounding the crack, see Figure 4. The x_i are coordinates at the crack tip but in the non-zoomed state, i.e. in case of the real specimen with adjacent interfaces [28]. In the zoomed coordinates, y_i, the influence of the adjacent laminate interfaces is not considered.

Change of the potential energy and Energy Release Rate calculation for combined (thermal and mechanical) loading

In order to predict the type of the further crack propagation (single or double crack penetration) and further propagation direction, the change of the potential energy $\delta\Pi_{a_p}$ or more precisely the so-called additional energy ΔW, released by the fracture process has to be calculated, as given by [27]:

$$\Delta W = \delta\Pi_{a_p} - G_c^{(M1)} a_p.$$ (2)

$G_c^{(M1)}$ is the critical energy release rate of material M1, which may be determined experimentally (see Table 1). The term $\delta\Pi_{a_p}$ expresses the change in the potential energy corresponding to a certain initial crack length increment, a_p. Calculation of ΔW is done for several crack increment lengths in all possible crack propagation directions. Then a direction (and type of propagation) is chosen, where the additonal energy ΔW reaches a maximal value.

Remark: Note that the Griffith-like condition (2) is only a necessary one and not sufficient one. The fracture process is possible if simultaneously the stress criterion is also fulfilled ($\sigma > \sigma_f$ - Table 1) [29, 30].

The change of the potential energy $\delta\Pi_{a_p}$ considering both the thermal and flexural sources of the stress is calculated by integration of the energy release rate along the crack increment as given by:

$$\delta\Pi_{a_p} = \int_0^{a_{p0}} G\, da_{p(b)} = W_S \int_0^{\varepsilon_0} \left(G^{(1)} + G^{(2)} + ... \right) d\varepsilon,$$ (3)

where W_S is the laminate height and G is the energy release rate for the given crack extension type. In case of a crack terminating at the interface of two dissimilar materials, the total energy release rate can be expressed in terms of the asymptotic expansion given by:

$$G = G^{(1)} + G^{(2)} + ... = \left(\sqrt{G_m^{(1)}} + \sqrt{G_r^{(1)}} \right)^2 + \left(G_m^{(2)} + G_r^{(2)} \right) + ... , \frac{G^{(2)}}{G^{(1)}} \rightarrow 0 \text{ for } \varepsilon \rightarrow 0. \qquad (4)$$

It is worth mentioning that there are two sources of stress, i.e. mechanical (*m*) and residual (*r*) which, separately applied, give the crack extension forces G_m and G_r. When both sources of stresses are applied together, then the crack extension force G is calculated according to Eq. (4) (more details in [31]). Hence, in our case, the first term of the total crack extension force due to the combined loading (flexural and thermal) is given by:

$$G^{(1)} = -W_S^{2\delta_1} \frac{2\delta_1}{2W_S} H_1^2 K_{1p(b)} \left(\varphi_p \right) \varepsilon^{2\delta_1 - 1} \cdot \Psi_1 - W_S^{\delta_1 + \delta_2} \frac{\delta_1 + d_2}{2W_S} H_1 H_2 \varepsilon^{\delta_1 + d_2 - 1} \cdot$$
$$\cdot \left(K'_{1p(b)} \left(\varphi_p \right) \cdot \Psi_1 + K_{2p(b)} \left(\varphi_p \right) \cdot \Psi_2 \right) - W_S^{2\delta_2} \frac{2\delta_2}{2W_S} H_2^2 K'_{2p(b)} \left(\varphi_p \right) \varepsilon^{2\delta_2 - 1} \cdot \Psi_2 \geq 0 \qquad (5)$$

The second term of the crack extension force due to the combined loading is for the case of the crack bifurcation given by

$$G^{(2)} = W_S^{1+\delta_1} \frac{\delta_1 + 1}{W_S} H_1 \sigma_{res}^{(M1)} \varepsilon^{\delta_1} \cos^2 \varphi_p \left(\int_0^{1/2} \mathcal{V}_{1y_1'} \left(y' \right) dy_2' + \int_0^{1/2} \mathcal{V}_{1y_1''} \left(y'' \right) dy_2'' \right) -$$
$$- W_S^{1+\delta_1} \frac{\delta_1 + 1}{W_S} H_1 \sigma_{res}^{(M1)} \varepsilon^{\delta_1} \sin \varphi_p \cos \varphi_p \left(\int_0^{1/2} \mathcal{V}_{1y_2'} \left(y' \right) dy_2' - \int_0^{1/2} \mathcal{V}_{1y_2''} \left(y'' \right) dy_2'' \right) +$$
$$+ W_S^{1+\delta_2} \frac{\delta_2 + 1}{W_S} H_2 \sigma_{res}^{(M1)} \varepsilon^{\delta_2} \cos^2 \varphi_p \left(\int_0^{1/2} \mathcal{V}_{2y_1'} \left(y' \right) dy_2' + \int_0^{1/2} \mathcal{V}_{2y_1''} \left(y'' \right) dy_2'' \right) -$$
$$- W_S^{1+\delta_2} \frac{\delta_2 + 1}{W_S} H_2 \sigma_{res}^{(M1)} \varepsilon^{\delta_2} \sin \varphi_p \cos \varphi_p \left(\int_0^{1/2} \mathcal{V}_{2y_2'} \left(y' \right) dy_2' - \int_0^{1/2} \mathcal{V}_{2y_2''} \left(y'' \right) dy_2'' \right) \gtreqless 0. \qquad (6)$$

For the case of the single crack deflection $G^{(2)}$ adopts the same form as Eq. (6), where only one integral (from 0 to 1 - for one branch) is considered within the brackets.

Note that GSIF or a T-stress is generally the sum of two contributions:

$$H_1 = H_1^m + H_1^r; \quad H_2 = H_2^m + H_2^r; \quad T = T^m + T^r, \qquad (7)$$

where H_i^m is due to pure flexural loading and H_i^r is due to pure thermal loading respectively. These parameters characterize the stress state in the crack tip vicinity. In case, when some of the GSIF (H_1 or H_2), are close (or equal) to 0 (e.g. case of the crack perpendicular to the interface), then the Eqs. (5) and (6) would significantly simplify.

The factors $K_{i\,p(b)} (\varphi_p)$ and the opening of the crack extension $\mathcal{V}_{2y_1'} \left(y' \right)$, $\mathcal{V}_{2y_2'} \left(y' \right)$, etc., are calculated by means of FEM on the inner domain once for all, since they depend only on the local geometry and material properties – for details see [25, 28].

RESULTS

Stress field description

The stress and displacement field, defined by Eq. (1), is now described for pure thermal and pure mechanical loading. Using the subsequent superposition, a combined loading can be obtained. A 2D FEM model of a laminate is developed (see Figure 5) with a crack terminating at the first ATZ/AMZ interface. In contrast with the experiment, no notch was modelled – only a straight crack which is a sufficient simplification of the problem. The total model height is 4.03 mm and it corresponds to the real specimen height, where a volume ratio V_{AMZ}/V_{ATZ} of 1/6.1 is achieved. Width of the 2D model is considered as unit together with element plane strain condition. The applied loading force F in FEM calculations is then always related to this unit width, i.e. in comparison with the experimental record in Figure 2a, is multiplied by factor 1/B.
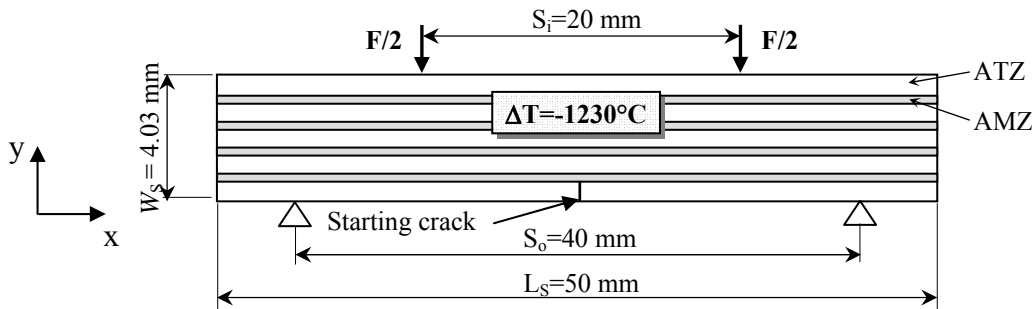

Figure 5. Scheme of a laminate used for the calculations.

Layer thicknesses were considered same as in a real specimen and were the following (from bottom): 773, 147, 616, 125, 623, 142, 634, 148, 819 μm. Vicinity of the crack tip was modelled with a very fine mesh (PLANE82 elements) and the crossings of the integration path with an interface were also refined to accurate capture the discontinuity by the stress σ_{xx} in this region. The element size at the crack tip was lower than 1μm. Radius of the circular integration path was chosen as R=7μm around the crack tip. Nevertheless, the choice of this radius plays no role on the computed GSIFs using the interaction integral [23,28]. The obtained solution of stresses and displacements was compared with the analytical singular field (1) based on the complex potentials, in order to determine a dominance domain of the singular terms. An example of such a comparison is shown in Figure 6, where a combined mechanical and thermal loading was simultaneously applied. In case of the thermal loading, the temperature change ΔT=-1230°C was applied to the FEM model (cooling down from the reference – stress free – temperature to room temperature). To simulate the mechanical (four point flexure) loading, the force F=10/B N was prescribed – as depicted in Figure 5 (this corresponds to the applied force F=10N on the real specimen of given width B – see Figure 2b).

94

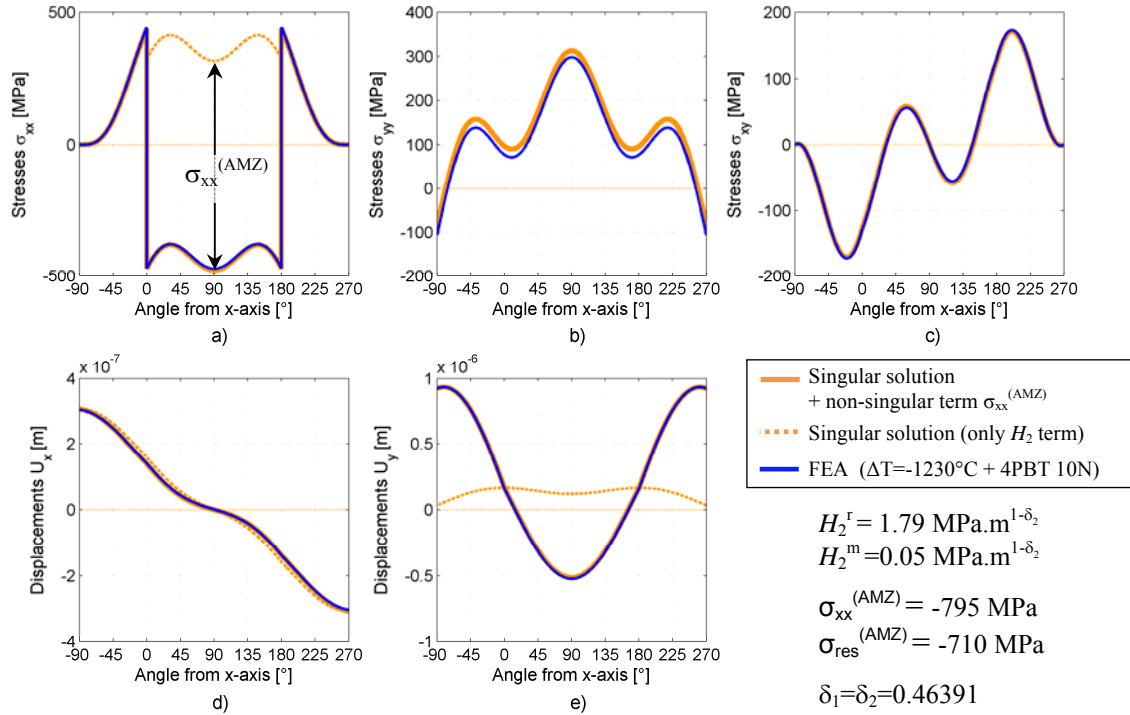Figure 6. Stresses and displacements for the combined loading (thermal + mechanical) on the circular path in the distance of R=7μm from the crack tip. ΔT=−1230°C and applied force is F=10N on the unit width of the specimen.

It can be concluded, from Figure 6, that for the case of a strong singularity a very good agreement between analytical and FE solution can be obtained – up to distance of circa R=40μm. Knowledge of this dominance distance is important with respect to the fracture criterion definition − to determine a distance from the crack tip, where the criterion (based only on the singular terms) is valid without any significant errors. The analytical definition of the non-singular term $\sigma_{xx}^{(AMZ)}$ can be found in [26].

Note, that for the case of a crack perpendicular to the interface one of the GSIFs is zero – thus $H_1^m = H_1^r = H_1 = 0$ (pure mode I loading). GSIF H for the arbitrary loading can be derived from one reference calculation - without need of other FE simulations (thanks to the linear dependency of GSIF on the applied load). GSIF for the combined loading is then a sum of the particular contributions – Eq.(7).

Crack path prediction

A competition between single crack penetration and crack bifurcation in case of the laminate defined in the previous section was investigated. Using Eqs. (3), (5) and (6) the change of the potential energy for several possible propagation directions was calculated and is represented in Figure 7. Both, length of the crack extension a_p and GSIF H_2^m were varied in a wide range of values. The crack extension a_p was varied in

order to be always smaller than the radius of the domain where the singular stress field (1) prevails.
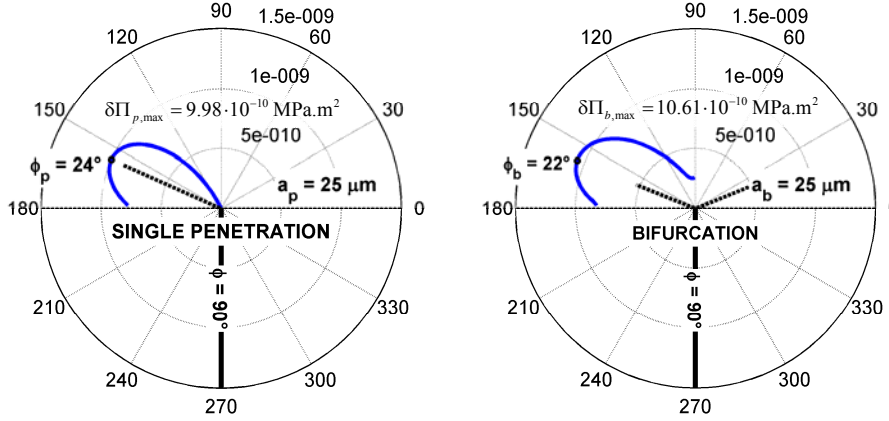

Figure 7. Variation of the change of the potential energy $\delta\Pi$ with the angle of the crack extension for a) single crack deflection and b) crack bifurcation. Crack extension length a_p=25µm, H_2^r=0.39 MPa.m$^{1-\delta_2}$ and H_2^m=1.1 MPa.m$^{1-\delta_2}$ (flexure load 220N).

The obtained numerical results showed that both crack bifurcation or crack deflection are preferred modes of fracture with respect to straight crack propagation. The angle of deflection/bifurcation, φ_p, was predicted to be in the range 20° – 30° which is in a good agreement with experimental observations. However, contrary to experimental data, the crack propagation was predicted even for the loading force about of 10 N, i.e. much lower value then the threshold value of 220 N found experimentally, see Figure 2. This discrepancy made us reexamine the real crack path. By inspection of the fractographic observations in Figure 3 it could be found that crack does not bifurcate and/or deflect just at the interface but at a distance $\Delta a \cong 25$ µm behind the interface. This is due to the energy accumulated in the system during the unstable crack propagation (in the ATZ layer which is subjected to tensile residual stress) before the crack reaches the interface. The accumulated energy allows the crack to penetrate inside the compressive layer. The stress field around the edge of the penetrating crack is square-root singular with the regular stress intesity factor K_I. It is worth mentioning that the radius of the dominance domain of the square-root singular field is only few microns as detailed numerical calculations revealed. Outside this domain the singular stress field (1) still prevails. However, it was found that the intensity of the singular stress field (1) caused by pure thermal loading, H_2^r, is significantly reduced. This is associated with the sharp change of residual stress between ATZ and AMZ layer. From linearity and dimensional considerations we can relate the GSIF H_2^r and the regular stress intesity factor K_I^r as:

$$K_I^r \Big/ \sqrt{t_{ATZ} + \Delta a} = k \cdot H_2^r \Big/ \left(t_{ATZ}\right)^{1-\delta_2} , \qquad (8)$$

where t_{ATZ} denotes the thickness of the ATZ layer and k is a dimensionless coefficient which describes the reduction of GSIF H_2^r. The coefficient k can be found from the

numerical calculations of K_I^r, specifically $k \cong 0.22$. If the reduction of GSIF H_2^r is applied in the crack deflection/branching analysis, a very good agreement with experimental data is obtained. Figure 7 shows that the crack branches/deflects at the angle $\varphi_p \cong 22°$ for the loading force $F \cong 220$ N when the additonal energy ΔW (see Eq. (2)) is starting to be greater than zero. It can be also inferred from Figure 7 that crack bifurcation is preferred to crack deflection, because the change of the potential energy $\delta\Pi$ during crack bifurcation is (slightly) greater than that corresponding to to single crack deflection.

The key feature in the design is the high residual compressive stress in the AMZ layer, which is present in laminate configurations with relative high material volume ratio (i.e. $V_{ATZ}/V_{AMZ} \geq 5$). In laminate configurations with lower volume ratios the residual stresses are lower and the inclined single penetration of the crack might be preferred to crack bifurcation.

CONCLUSIONS

A semi-analytical model based on Finite Fracture Mechanics theory has been developed to describe and predict the crack propagation (i.e. straight propagation, single deflection or bifurcation) in layered ceramics during flexural loading. Results have been compared with experiments in an alumina-zicronia multilayer ceramic designed with internal residual stresses. A combined loading (thermal and mechanical) has been taken into consideration to clarify the influence of the residual stresses on the crack path during fracture.

The proposed fracture criterion, where the crack follows the path which maximizes the energy released in the fracture process, can predict both the type and angle of propagation of a crack through the interface in a layered structure. For the laminate of study, crack bifurcation observed in experiments can be explained with the proposed model. The key feature in the design is the high residual internal stresses in the compressive layers which favour the propagation of the crack through the interface between layers at an inclined angle.

ACKNOWLEDGEMENTS

REFERENCES

1. Clegg, W.J., Kendall, K., Alford, N.M., Button, T.W., Birchall, J.D. (1990) *Nature* **347,** 455-7.
2. Padture, N.P., Lawn, B.R. (1994) *J. Am. Ceram. Soc.* **77,** 2518-22.
3. Prakash, O., Sarkar, P., Nicholson, P.S. (1995) *J. Am. Ceram. Soc.* **78,** 1125-7.
4. Marshall, D.B., Morgan, P., Housley, R.M. (1997) *J. Am. Ceram. Soc.***80,** 1677-83.
5. Clegg, W.J. (1998) *Materials Science and Technology* **14,** 486-95.
6. Li, D., Qiao, G., Jin, Z. (2004) *Ceramics International* **30,** 213-7.
7. Ceylan, A., Fuierer, P.A. (2007) *Materials Letters* **61,** 551-5.
8. Tomaszewski, H., Weglarz, H., Wajler, A., Boniecki, M., Kalinski, D. (2007) *J. Am. Ceram. Soc.* **27,** 1373-7.
9. Marshall, D.B., Ratto, J.J., Lange, F. (1991) *J. Am. Ceram. Soc.* **74,** 2979-87.
10. Russo, C.J., Harmer, M.P., Chan, H.M., Miller, G.A. (1992) *J. Am. Ceram. Soc.* **75,** 3396-400.
11. Sanchez-Herencia, J., Moya, J., Tomsia, A. (1998) *Scripta Materialia* **38,** 1-5.
12. Moon, R.J., Bowman, K.J., Trumble, K.P. (2001) *Acta Materialia* **49,** 995-1003.
13. Lakshminarayanan, R., Shetty, D.K. (1996) *J. Am. Ceram. Soc.* **79,** 79-87.
14. Rao, M., Sanchez-Herencia, J., Beltz, G., McMeeking, R.M., Lange, F. (1999) *Science* **286,** 102-5.
15. Pascual, J., Chalvet, F., Lube, T., De Portu, G. (2005) *Materials Science Forum* **492-493,** 581-6.
16. Sglavo, V., Paternoster, M., Bertoldi, M. (2005) *J. Am. Ceram. Soc.* **88,** 2826-32.
17. Lugovy, M., Slyunyayev, V., Orlovskaya, N., Blugan, G., Kübler, J., Lewis, M.H. (2005) *Acta Materialia* **53,** 289-96.
18. Šajgalik, P., Lences, Z., Dusza, J. (2006) *Composites Part B* **37,** 515-23.
19. Bermejo, R., Torres, Y., Baudin, C., Sánchez-Herencia, A.J., Pascual, J., Anglada, M. et al. (2007) *J Eur Ceram Soc* **27,** 1443-8.
20. Jianxin, D., Zhenxing, D., Dongling, Y., Hui, Z., Xing, A., Jun, Z. (2010) *Materials Science and Engineering: A* **527,** 1039-47.
21. Bermejo, R., Danzer, R. (2010) *Eng Fract Mech* **77,** 2126-35.
22. He, M., Evans, A.G., Hutchinson, J.W. (1994) *Int.J. Sol. and Struct.* **31,** 3443-55.
23. Profant, T., Ševeček, O., Kotoul, M. (2008) *Eng. Fract. Mech.* **75,** 3707-26.
24. Desmorat, R., Leckie, F.A. (1998) *Eur. J. of Mechanics - A/Solids* **17,** 33-52.
25. Kotoul, M., Ševeček, O., Profant, T. (2010) *Eng Fract Mech* **77,** 229-48.
26. Kotoul, M., Ševeček, O., Vysloužil, T. (2011) *AES-ATEMA 2011, Italy*.
27. Martin, E., Leguillon, D., Lacroix, C. (2001) *Composites Sci Technol* **61,** 1671-9.
28. Ševeček, O., Kotoul, M., Profant, T. (2012) *Eng Fract Mech* **80,** 28-51.
29. Taylor, D. The Theory of Critical Distances. Elsevier 2007.
30. Leguillon, D. (2002) *European Journal of Mechanics - A/Solids* **21,** 61-72.
31. Tada, H., Paris, P.C., Irwin, G.R. (1985) *The stress analysis of cracks handbook,* Del Research, St. Louis, MO, USA.